[redacted] SECURITY INFORMATION

Copy 202
RM L52F23

NACA

RESEARCH MEMORANDUM

PRELIMINARY FREE-FLIGHT INVESTIGATION OF THE ZERO-LIFT DRAG PENALTIES OF SEVERAL MISSILE NOSE SHAPES FOR INFRARED SEEKING DEVICES

By Robert O. Piland

Langley Aeronautical Laboratory
Langley Field, Va.

[redacted]

[redacted]

[redacted]

NATIONAL ADVISORY COMMITTEE
FOR AERONAUTICS

WASHINGTON

December 9, 1952

[redacted]

[redacted]

Classification cancelled (or changed to UNCLASSIFIED)

By Authority of NASA Tech Pub Announcement #121
(OFFICER AUTHORIZED TO CHANGE)

By ..... 4 Oct 67
NAME AND

GRADE OF OFFICER MAKING CHANGE)

30 March 61
DATE

NATIONAL ADVISORY COMMITTEE FOR AERONAUTICS

RESEARCH MEMORANDUM

PRELIMINARY FREE-FLIGHT INVESTIGATION OF THE ZERO-LIFT DRAG PENALTIES OF SEVERAL MISSILE NOSE SHAPES FOR INFRARED SEEKING DEVICES

By Robert O. Piland

SUMMARY

The initial results of an investigation to study nose shapes considered suitable for housing an infrared seeker are presented. The zero-lift drag characteristics of a missile-like body with various unconventional nose shapes were obtained through a range of Mach numbers from 0.8 to 1.8 and Reynolds numbers, based on body length, from 20×10^6 to 70×10^6, respectively, by using rocket-propelled free-flight models. Results of the tests indicate that at supersonic speeds about 70 percent of the drag penalty incurred by using a spherical tip nose shape may be eliminated by using nose shapes which, it is believed, will still allow the seeker to function.

Of the nose shapes tested, a 30° cone incurred the smallest drag penalty at supersonic speeds when compared with parabolic nose shape of higher fineness ratio. Of those nose shapes which could possibly be constructed entirely of metal or of a transparent material, the differences in drag were negligible.

INTRODUCTION

In the present development of guidance systems for missiles, a seeker device, sensitive to infrared radiation, as described in reference 1, is being considered. A seeker of this type utilizes a lens, the preferable location of which is the nose of the missile. If the lens is located in the nose of the missile, however, the use of a low-drag parabolic or conical nose shape of high fineness ratio may be impractical because of aberrations and a high percentage of reflections. On the other hand, using the rather blunt lens or a spherical tip for a nose shape results in extreme drag penalties at Mach numbers above

about 1.4 as indicated in reference 2. The problem, therefore, resolves into one of determining a nose shape which will allow the seeker to operate but will not incur an intolerable drag penalty. Many nose shapes have been suggested by various sources as possible solutions to the problem. The possibilities of using plain spikes ahead of blunt bodies for drag reduction have been reported in references 3 and 4. The present investigation undertakes to assay the drag penalties which would be incurred by the use of several other suggested noses. The nose shapes were flight-tested on a fin-stabilized missile-like body. The models were rocket-propelled to a Mach number of 1.8. During the following coasting period, zero-lift drag data were obtained. The Reynolds number, based on body length, varied from 20×10^6 to 70×10^6 for Mach numbers from 0.8 to 1.8, respectively. Tests were conducted at the Pilotless Aircraft Research Station at Wallops Island, Va.

MODELS

Test Body

A photograph of the body on which the various nose shapes were flight-tested is shown in figure 1 with the basic parabolic nose. A drawing, with the body coordinates, is presented in figure 2(a). The body was fin-stabilized and 75 inches in length with a fineness ratio of 15. The body was made of mahogany and coated with red Phenoplast which was smoothly finished. The Phenoplast was used in order to maintain a high degree of smoothness at the temperatures encountered during flight testing. The polished duralumin fins were of hexagonal section with a maximum thickness of 0.25 inch.

The seeker lens was considered to be located at station 7.65 which gave a ratio of lens diameter to maximum body diameter of 3 to 5. All changes in nose shape were made ahead of this station, the lens location being fixed.

Nose Shapes

Parabolic nose.- As mentioned previously, the ideal nose shape from the viewpoint of aerodynamic drag is currently considered to be impractical for use as a housing for an infrared seeker. Such a nose shape shown in figures 1 and 2(a) was tested for purposes of comparison.

Spherical nose.- The spherical nose shape, shown in figures 2(a) and 3(a), on the other hand, would have acceptable characteristics for a seeker standpoint but would be poor when considered aerodynamically.

This nose was tested since it was considered the shape giving the highest drag that a designer might tolerate.

The 30° conical nose.- It is believed (ref. 5) that for a conical nose the minimum apex angle which could be used in front of a seeker at the present time is about 30°. The nose shape tested as a result is shown in figures 2(a) and 3(b).

The 12-sided nose.- A 30° cone nose modified to have 12 sides is being considered for use with an optical guidance system such as that described in reference 6. Consideration has also been given to use of a 12-sided nose constructed of quartz with an infrared seeker. Consequently, the 12-sided nose shape shown in figures 2(a) and 3(c) was selected for testing.

Spike-mounted windshield.- Both the conical and 12-sided nose require the use of a material such as quartz, plastic, or glass through which the radiation from a target would pass before striking the lens. There is also the possibility of allowing at least a part of the radiation to reach the lens directly or, at most, to pass through only a sphere for which transmittance properties are excellent. Such a shape would be a spike-mounted windshield (figs. 2(a) and 3(d)) for which drag reduction possibilities were first pointed out by Robert T. Jones of the National Advisory Committee for Aeronautics and later confirmed by rocket tests in reference 7. The windshield consists of a cone with half-apex angle of 10° mounted on a truncated cone of 21° half angle. The ratio of windshield frontal area to lens area is 1 to 9.

Slotted cone.- A hollow 30° cone was modified (at the suggestion of Edmund C. Buckley of the NACA) by the removal of 50 percent of the surface area of the cone in the form of longitudinal strips. The nose shown in figures 2(a), 2(b), and 3(e) is the result. The infrared rays could enter the slots, and could also pass through the shielded parts if such parts were made of a transparent material, whereas it was hoped the slotted cone might retain the aerodynamic characteristics of the solid cone.

Slotted cone with 40° windshield.- The slotted-cone nose was modified by the addition of a 40° conical windshield. This configuration is shown in figures 2(a) and 3(f).

Ring nose.- From the slotted-cone and windshield noses was derived the ring nose shown in figures 2(a), 2(b), and 3(g). It is a hollow 30° cone modified by the removal of lateral strips in the amount of 50 percent of the surface area and is equipped with a small 50° conical windshield. This nose could be considered a succession of windshields or a slotted cone with lateral rather than longitudinal stringers. As in the case of the slotted cone, the infrared could pass through the

open lateral strips as well as through the shielded parts if these parts were made of transparent material.

PREFLIGHT JET TESTS

Since it was impractical to analyze the flow conditions about the slotted-cone and ring nose shapes, there was some concern about their ability to withstand the forces to which they would be subjected in flight. These nose shapes, therefore, were tested at $M = 1.8$ (in a jet with open test section), as described in reference 8. In addition to the structural tests, shadowgraphs were taken of the slotted cone with various conical windshields and the ring nose with a 50° conical windshield. A shadowgraph was also taken of the flow about the spike-mounted windshield. These shadowgraphs are presented in figures 4(a) to 4(f) to show the type of flow over the various nose configurations.

FLIGHT TESTS

A typical model ready for firing is shown in figure 5. As shown, the test models employed a two-stage propulsion system consisting of a 3.25-inch MK 7 rocket motor as the sustainer unit and a 5.0-inch rocket motor as the booster unit, the latter being equipped with stabilizing fins. The booster motor propelled the combination to a Mach number of about 1.1, and after separation the sustainer fired to bring the model to maximum Mach number. The drag data were obtained during the period of coasting flight subsequent to sustainer burnout. The Reynolds numbers encountered during this period are plotted against Mach number in figure 6. The flight tests covered a range of Reynolds numbers from 20×10^6 to 70×10^6 and Mach numbers from 0.8 to 1.8.

The drag data were obtained and reduced by the methods described in reference 9. The data were then corrected for the effects of winds at altitude. The instrumentation consisted of Doppler radar, a modified SCR 584 radar set, and radiosonde. Drag coefficients are based on body frontal area and each represents the total drag of the configuration. Figure 7 presents the variation of drag coefficient with Mach number for a typical model showing the continuity of the data points. The errors in drag coefficient and Mach number are believed to be less than ± 0.01.

RESULTS OF FLIGHT TESTS AND DISCUSSION

The results of the flight tests are presented as the variation of total drag coefficient with Mach number in figures 8 to 11. The penalizing effect of rounding the nose is seen in figure 8 and the seriousness of the problem is emphasized by these results. All the noses considered to be possibly suitable for seeker housing reduced this drag penalty greatly. The 30° cone nose shape offered the most effective means of drag reduction; its increase in drag over the basic parabolic nose being due partly to decreased fineness ratio. The drag coefficient of the 12-sided nose (fig. 9) was practically the same as that of the conical nose throughout the Mach number range. It is of interest to note the late drag rise Mach number of these two models. No attempt is made to explain this phenomenon at the present time and further information will be necessary before this subject can be clarified.

The remaining nose shapes were all only slightly less effective in reducing the drag of the spherical-tip nose than the conical nose at supersonic speeds. Unpublished test results indicate that other combinations of windshields and spike lengths than those tested here may result in greater drag reduction. The effect of equipping a slotted cone with a 40° conical windshield (fig. 11) is small but favorable.

The present tests, although encouraging, are far from conclusive from an over-all standpoint. Further testing is necessary to study the characteristics of these shapes under lifting conditions, as well as to determine with an actual seeker their suitability for seeker housing.

CONCLUSIONS

The results of a preliminary investigation to study nose shapes considered to be suitable for housing an infrared seeker and offering a minimum of aerodynamic penalties are presented. The variation of zero-lift drag with Mach number for a missile-like body with various nose shapes indicates the possible use of several noses constructed from either transparent or nontransparent (metal) material. Specifically, the following conclusions were drawn from flight-test results:

1. Of the nose shapes tested, the 30° conical and the 12-sided nose shapes incurred the smallest drag penalty as compared to the parabolic nose shape at supersonic speeds.

2. Of the nose shapes that could be constructed of metal, as well as a transparent material, the differences in drag were negligible.

Langley Aeronautical Laboratory,
National Advisory Committee for Aeronautics,
Langley Field, Va.

REFERENCES

1. Sevadjian, Edward M., Mleczko, Eugene L., Bunker, Earle R., Jr.: Final Engineering Summary Report on the Development of Infrared Homing Set AN/DAN-s(XN-1) Rep. No. 2056, Contract NOa(s) 10231, Item 5, Bur. Aero., Gen. Tire and Rubber Co. of Calif. (Azusa), Dec. 22, 1950.

2. Hart, Roger G.: Flight Investigation of the Drag of Round-Nosed Bodies of Revolution at Mach Numbers From 0.6 to 1.5 Using Rocket-Propelled Test Vehicles. NACA RM L51E25, 1951.

3. Moeckel, Wolfgang E.: Flow Separation Ahead of a Blunt Axially Symmetric Body at Mach Numbers 1.76 to 2.10. NACA RM E51I25, 1951.

4. Jones, Jim J.: Flow Separation From Rods Ahead of Blunt Noses at Mach Number 2.72. NACA RM L52E05a, 1952.

5. Snow, O. J.: The Development of Irdomes. Progress Rep. Oct 1, 1950 to June 1, 1951. Rep. No. NADC-EL-5107, Bur. Aero. TED Project No. ADS EL-889, Aeronautical Electronic and Electrical Lab., U. S. Naval Air Dev. Center. Oct. 11, 1951.

6. Anon: Optical System for Target Seekers, Supersonic Missiles. Contract W33-038-ac-17618, [U. S. Air Force], Farrand Optical Co., Inc. (New York), 1949.

7. Alexander, Sidney R., and Katz, Ellis: Flight Tests To Determine the Effect of Length of a Conical Windshield on the Drag of a Bluff Body at Supersonic Speeds. NACA RM L6J16a, 1947.

8. Faget, Maxime A., Watson, Raymond S., and Bartlett, Walter A., Jr.: Free-Jet Tests of a 6.5-Inch-Diameter Ram-Jet Engine at Mach Numbers of 1.81 and 2.00. NACA RM L50L06, 1951.

9. Welsh, Clement J.: Results of Flight Tests To Determine the Zero-Lift Drag Characteristics of a 60° Delta Wing With NACA 65-006 Airfoil Section and Various Double-Wedge Sections at Mach Numbers From 0.7 to 1.6. NACA RM L50F01, 1950.

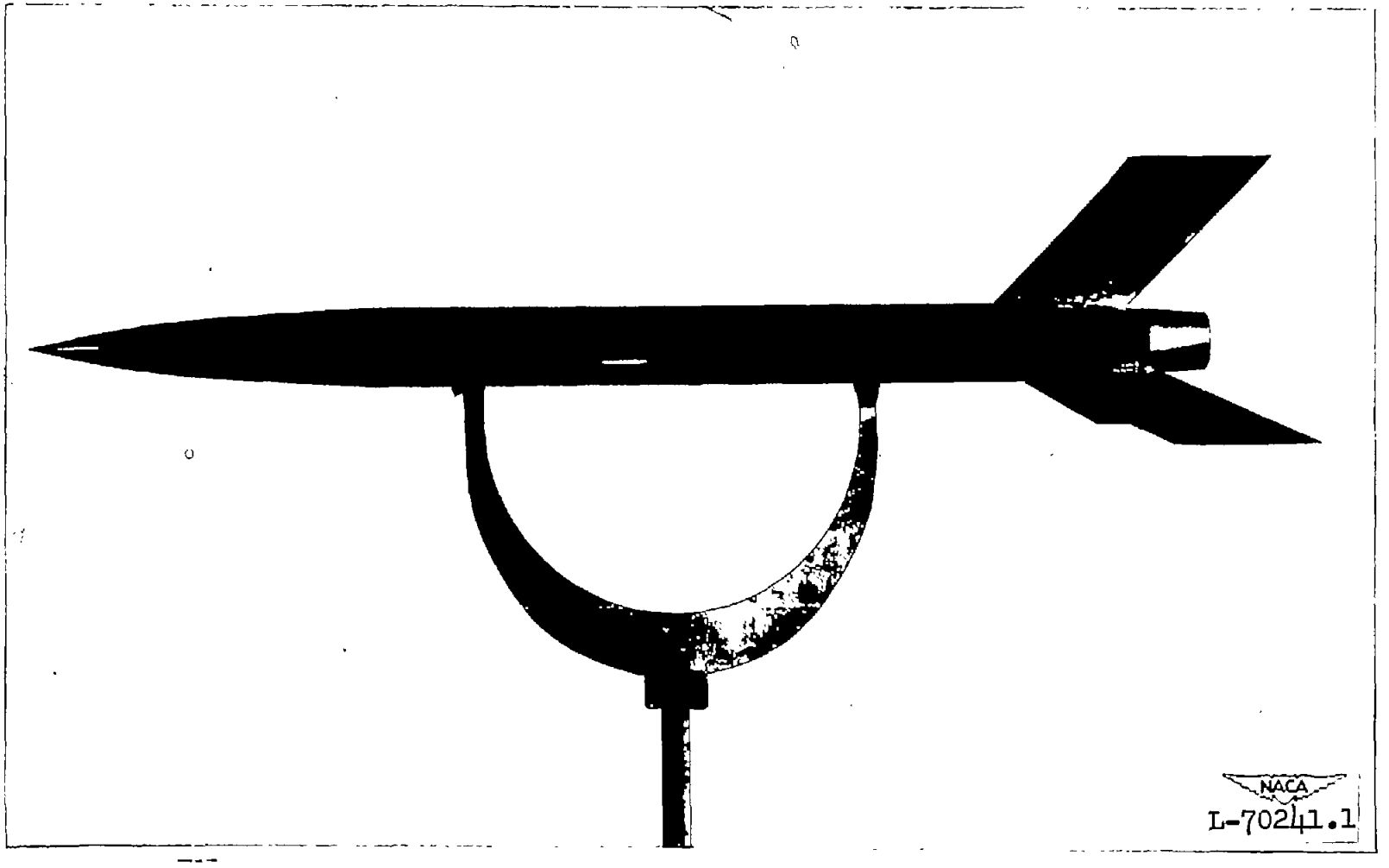

Figure 1.- Test body with basic parabolic nose shape.

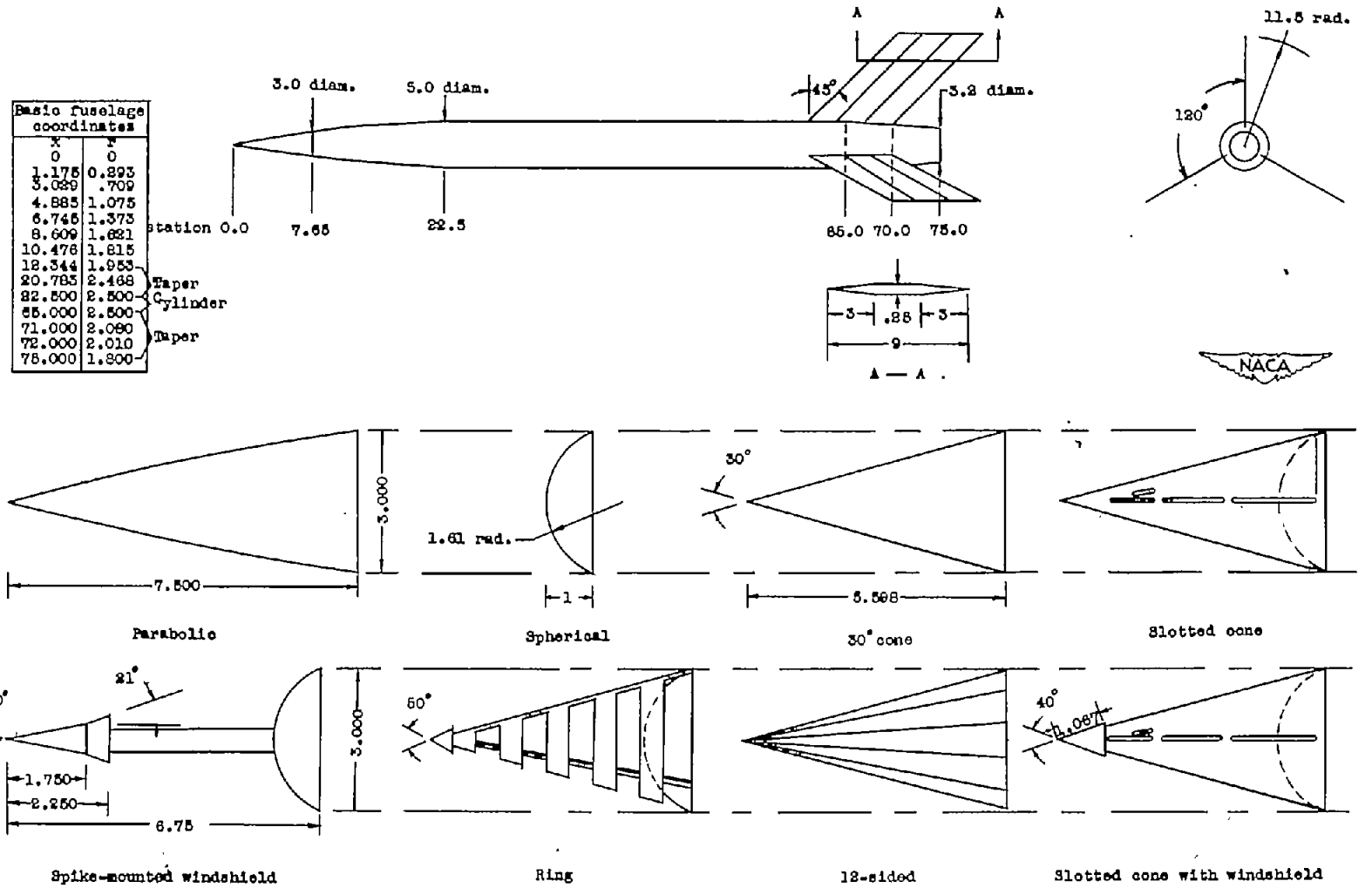

(a) General views. Dimensions are in inches.

Figure 2.- Test configurations.

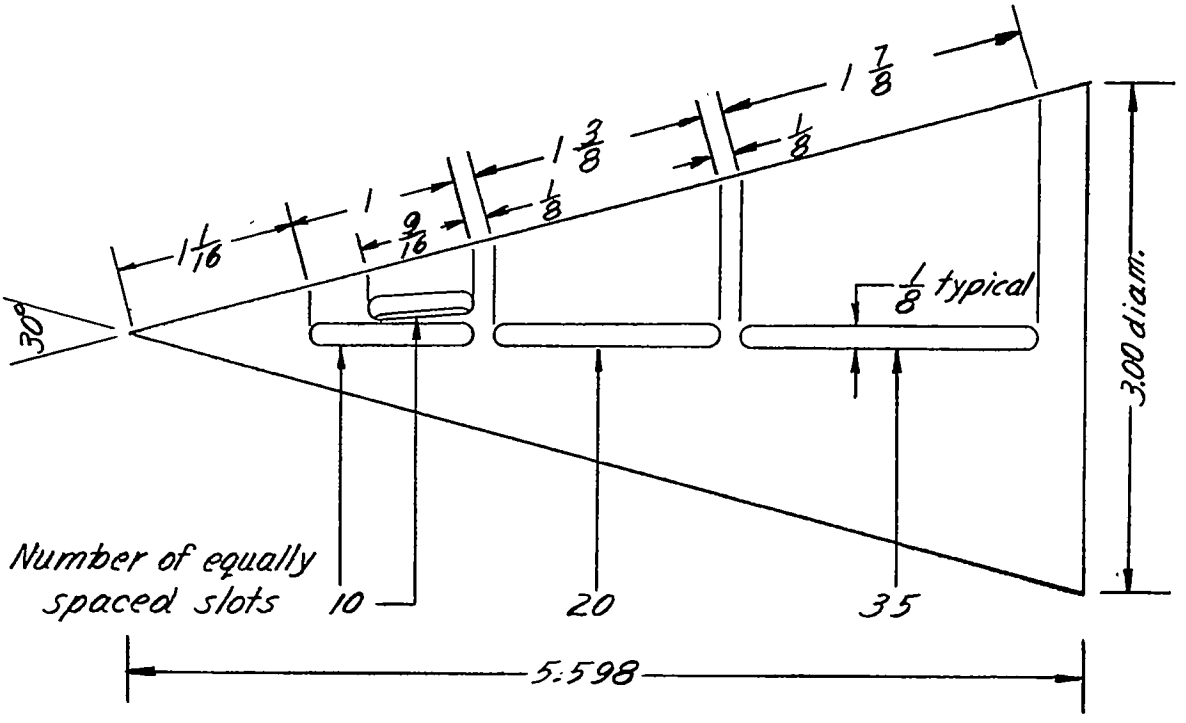

Slotted cone nose

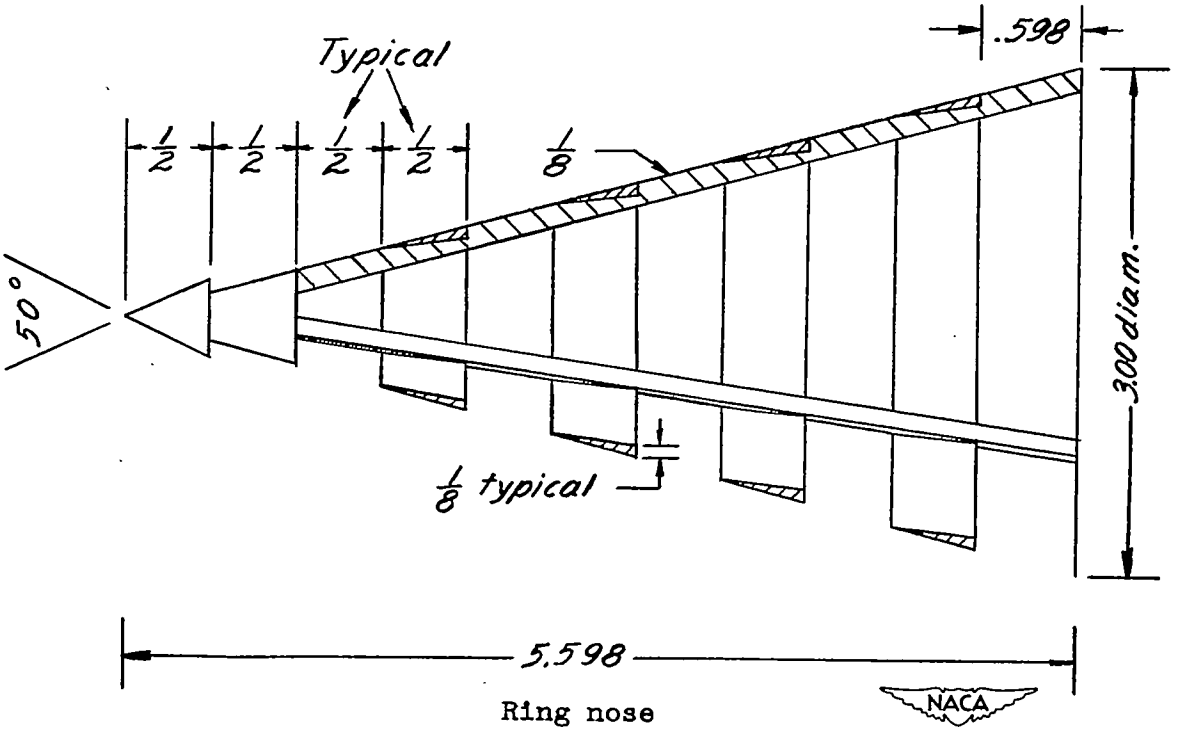

Ring nose

(b) Detailed drawing of slotted-cone and ring nose shapes. Dimensions are in inches.

Figure 2.- Concluded.

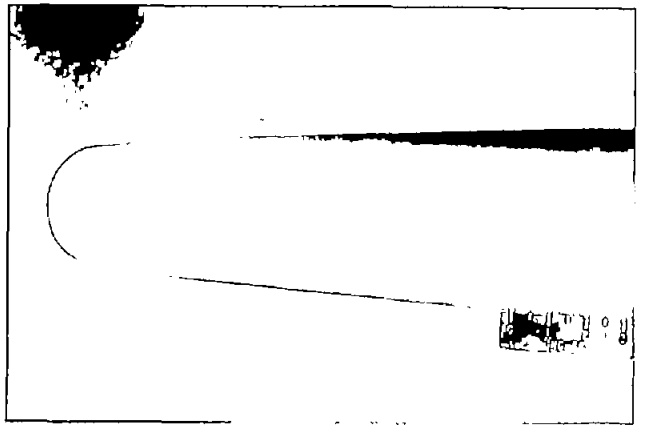

(a) Spherical nose.

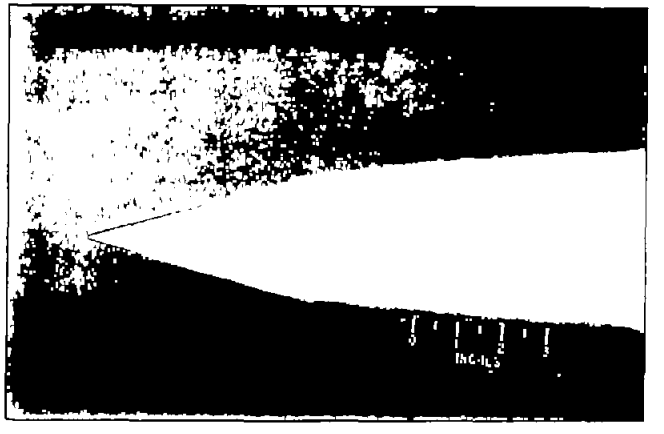

(b) The 30° conical nose.

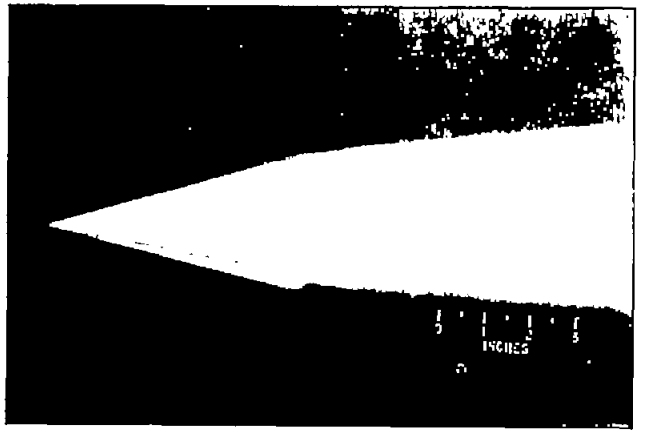

(c) The 12-sided nose.

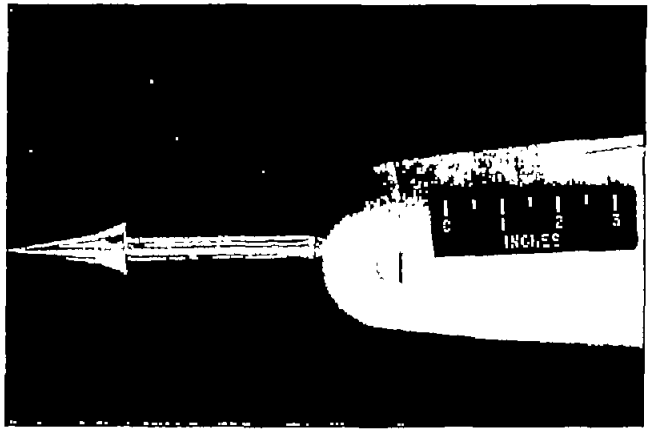

(d) Spike-mounted windshield.

NACA

L-75144

Figure 3.- Nose shapes tested.

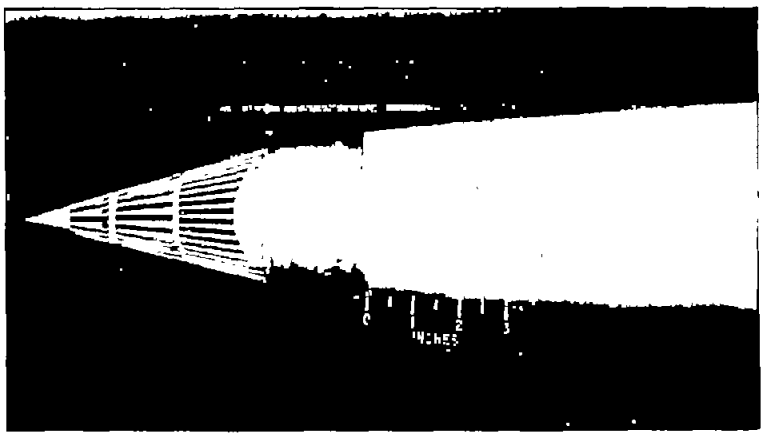

(e) Slotted cone.

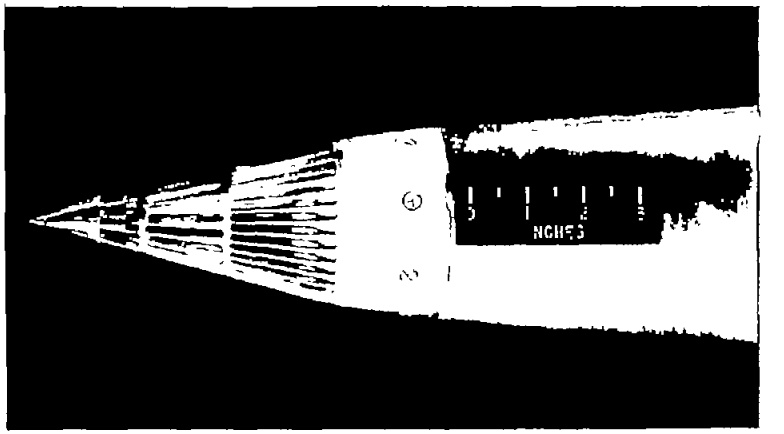

(f) Slotted cone with 40° windshield.

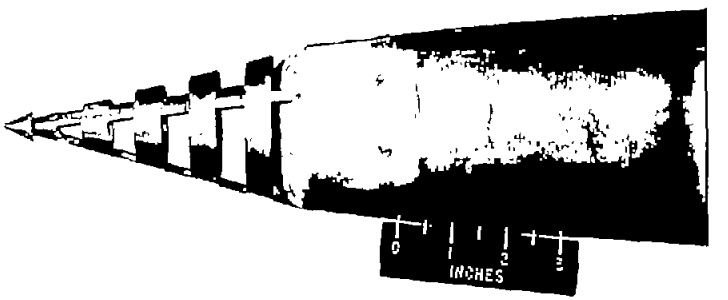

(g) Ring nose.

NACA L-75145

Figure 3.- Concluded.

(a) Spike-mounted windshield.

(b) Slotted cone.

NACA
L-75146

Figure 4.- Shadowgraphs of various nose shapes at a Mach number of 1.8.

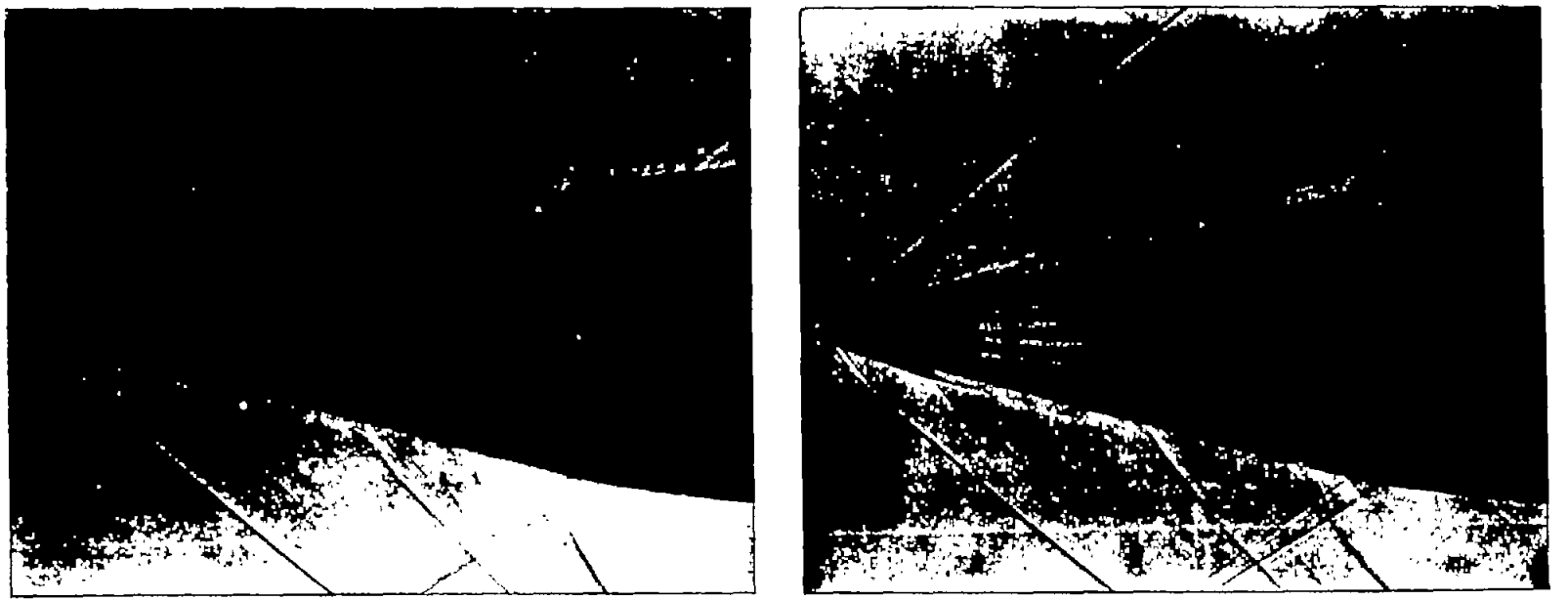

(c) Slotted cone with short 40° windshield (not flight tested). (d) Slotted cone with long 40° windshield.

NACA
L-75147

Figure 4.- Continued.

(e) Slotted cone with 50° windshield (not flight tested).

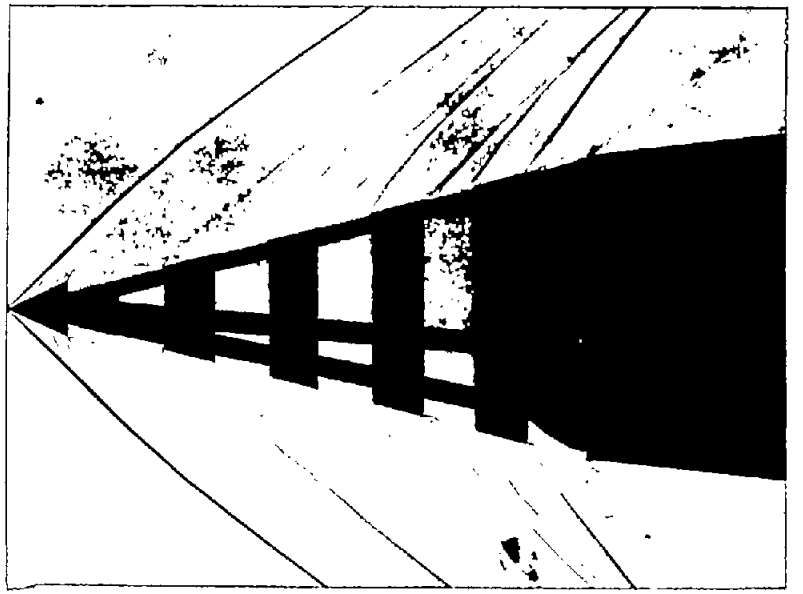

(f) Ring nose with 50° windshield.

NACA
L-75148

Figure 4.- Concluded.

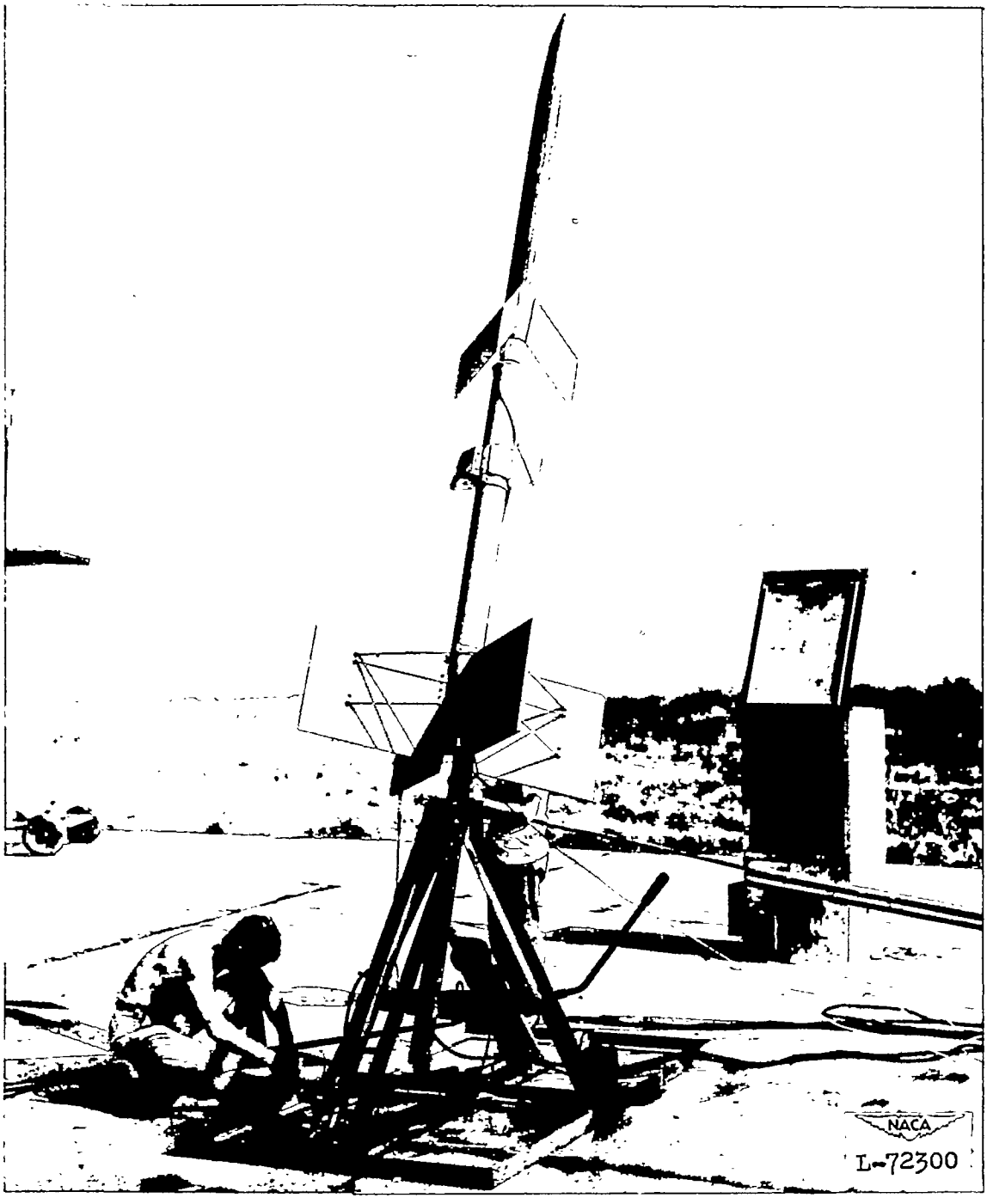

Figure 5.- Model in position for launching.

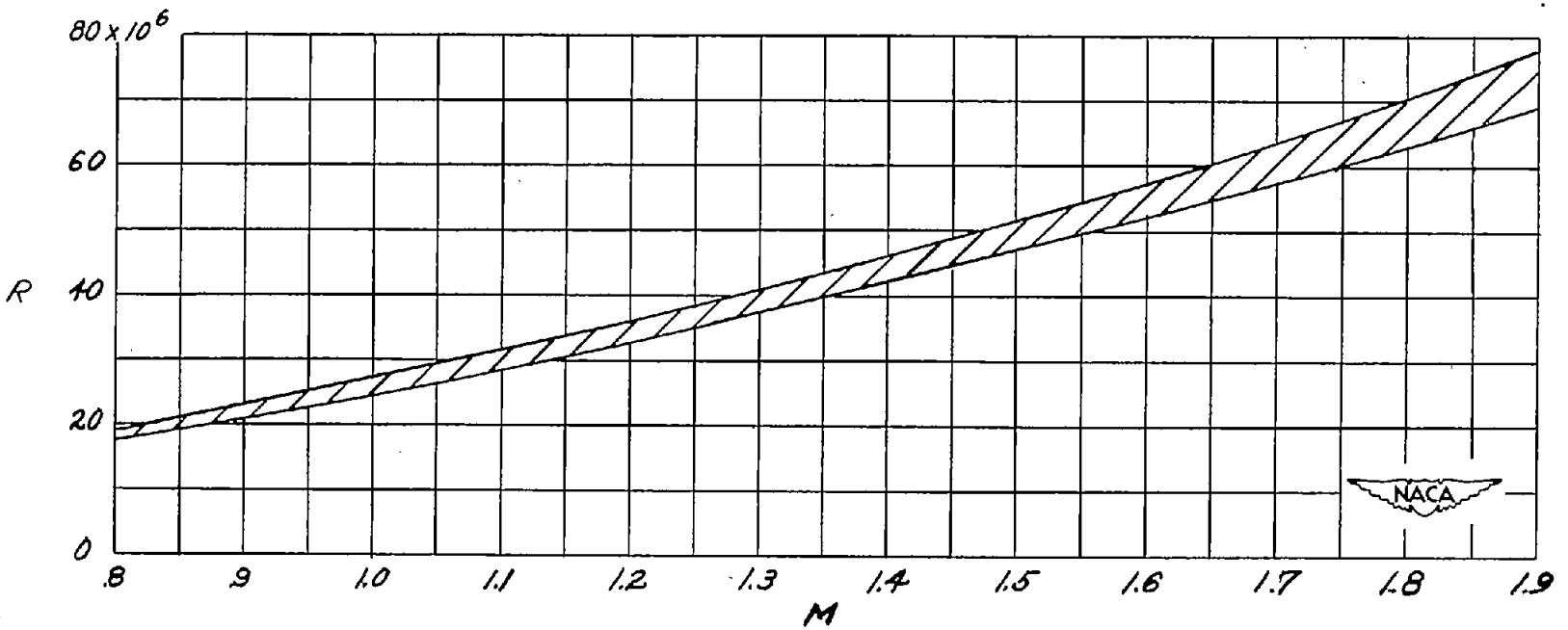

Figure 6.- Reynolds number R based on body length plotted against Mach number M.

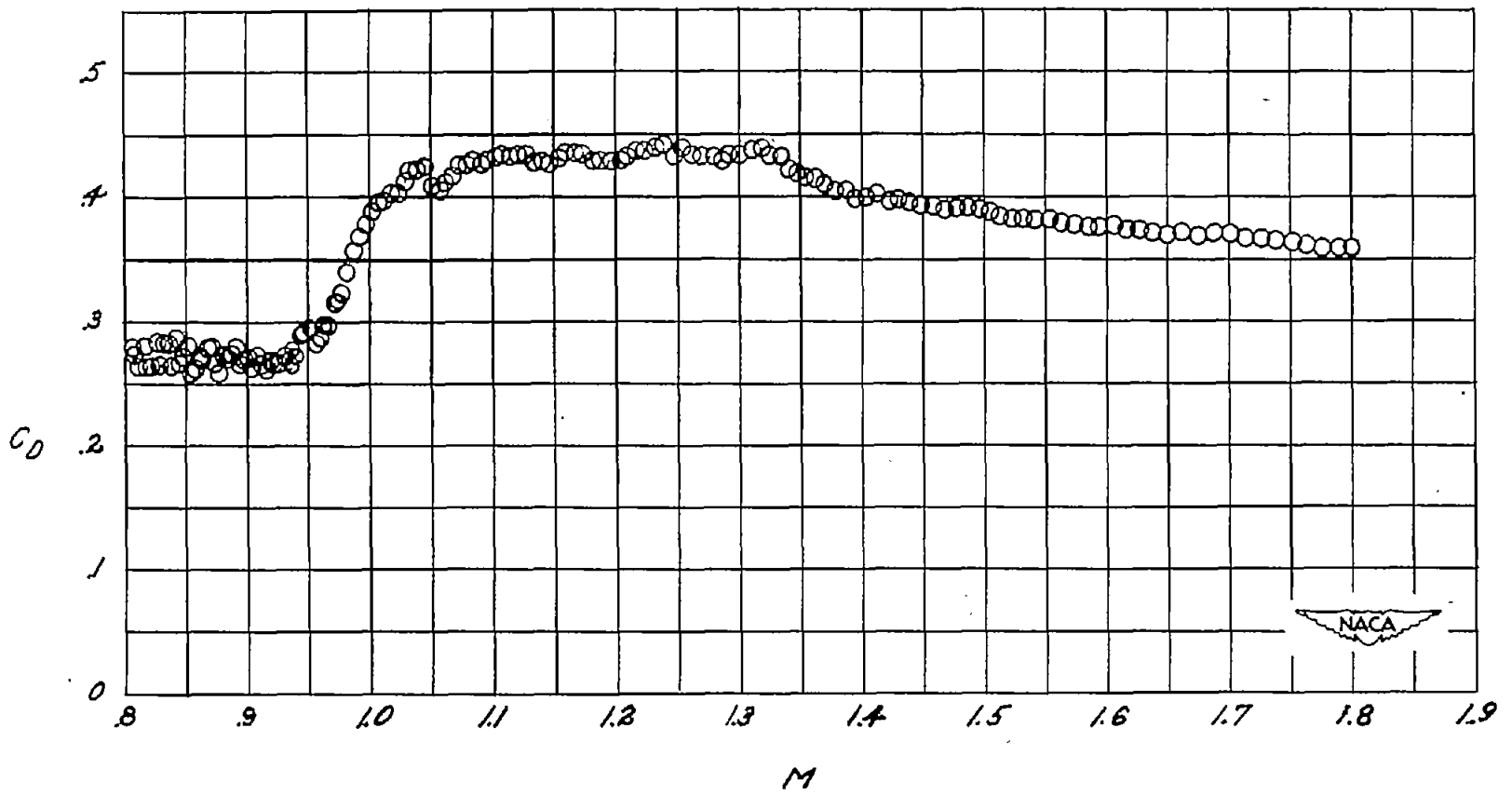

Figure 7.- Variation of total drag coefficients with Mach number for a typical model showing calculated data points.

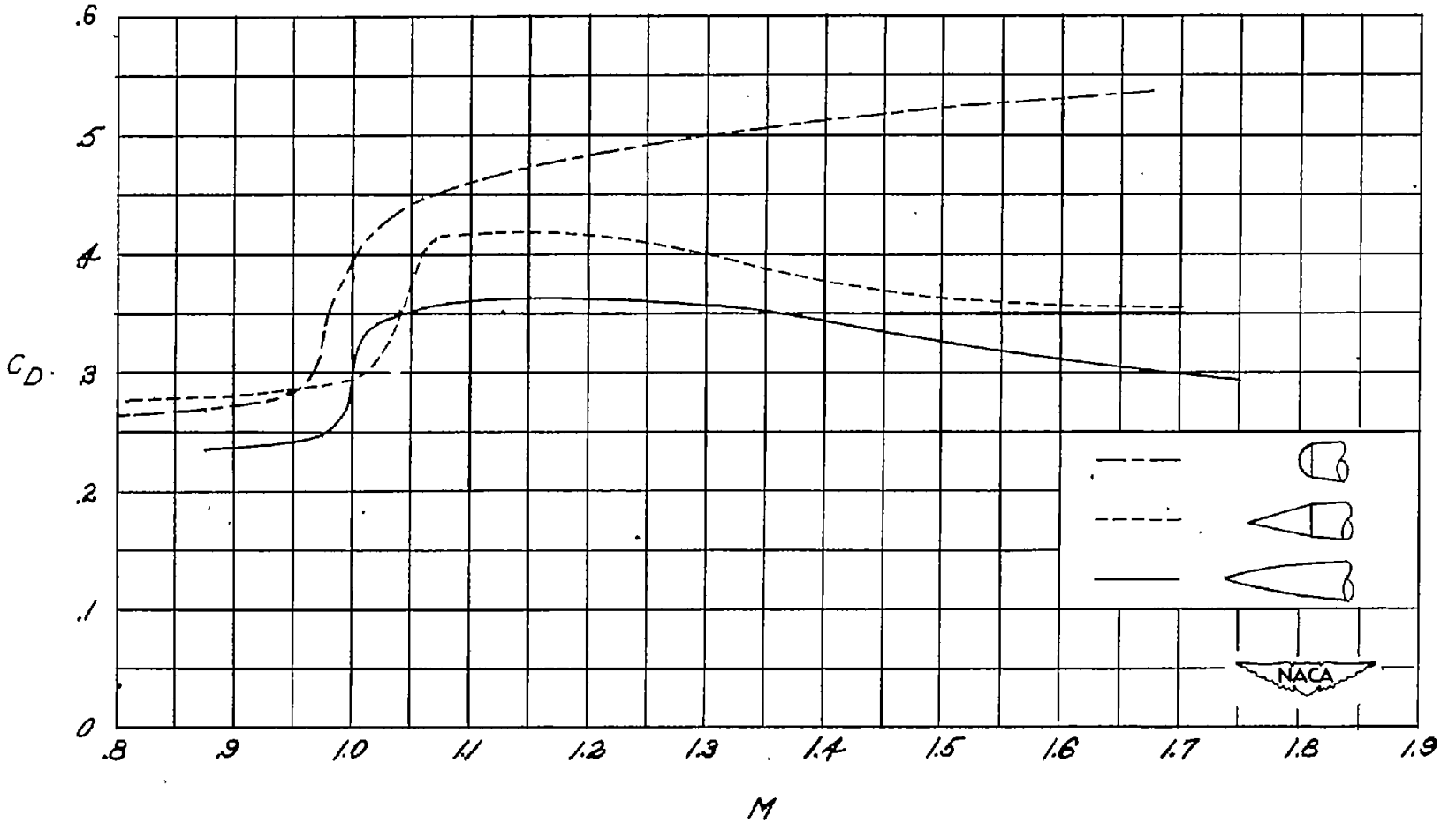

Figure 8.- Drag coefficient based on body frontal area C_D plotted against Mach number M for the basic parabolic, 30° cone, and spherical nose shapes.

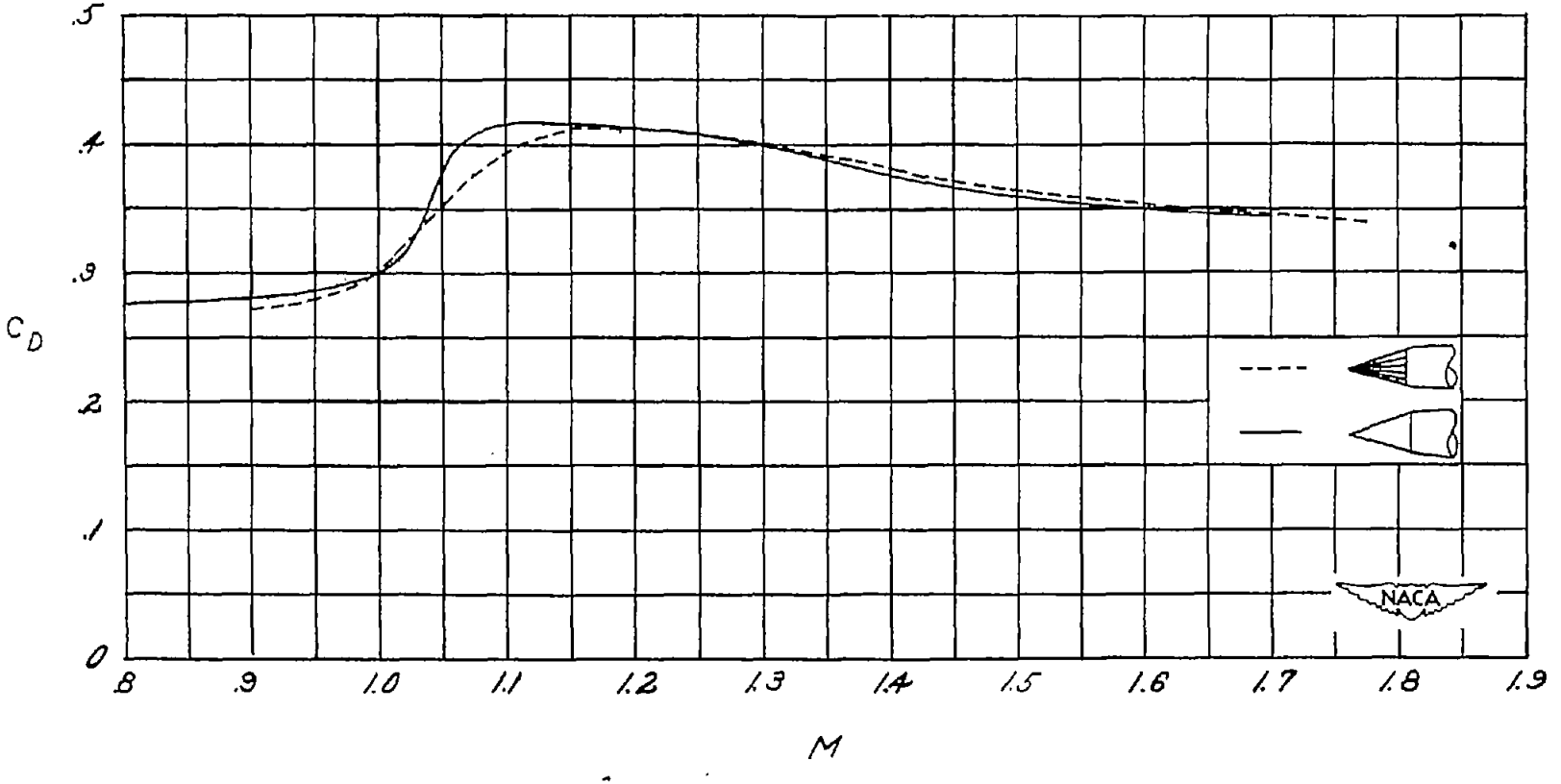

Figure 9.- Drag coefficient based on body frontal area C_D plotted against Mach number M for models with 30° cone and 12-sided nose shapes.

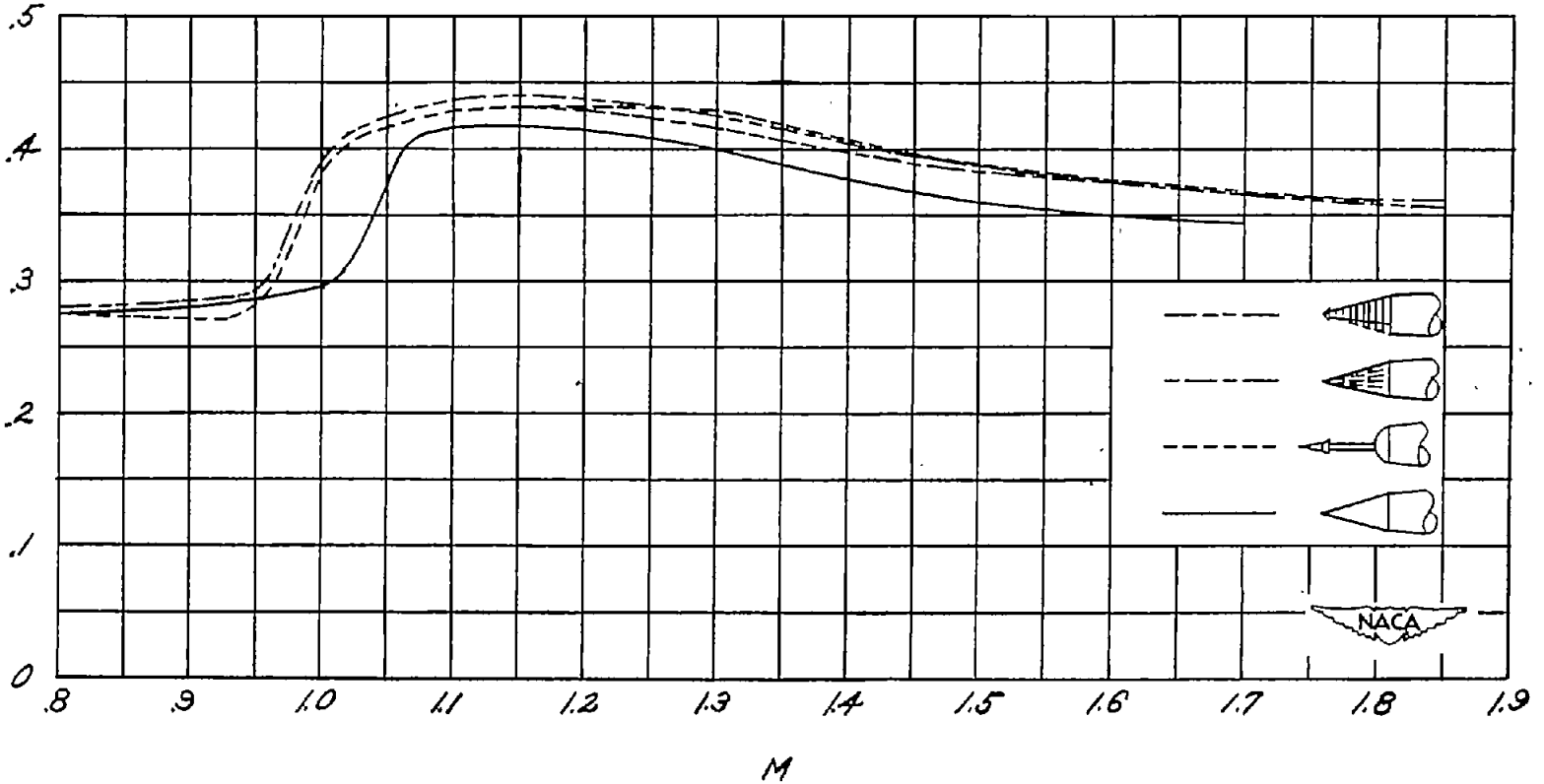

Figure 10.- Drag coefficient based on body frontal area C_D plotted against Mach number M for models with 30° cone, spike-mounted windshield, slotted-cone and ring nose shapes.

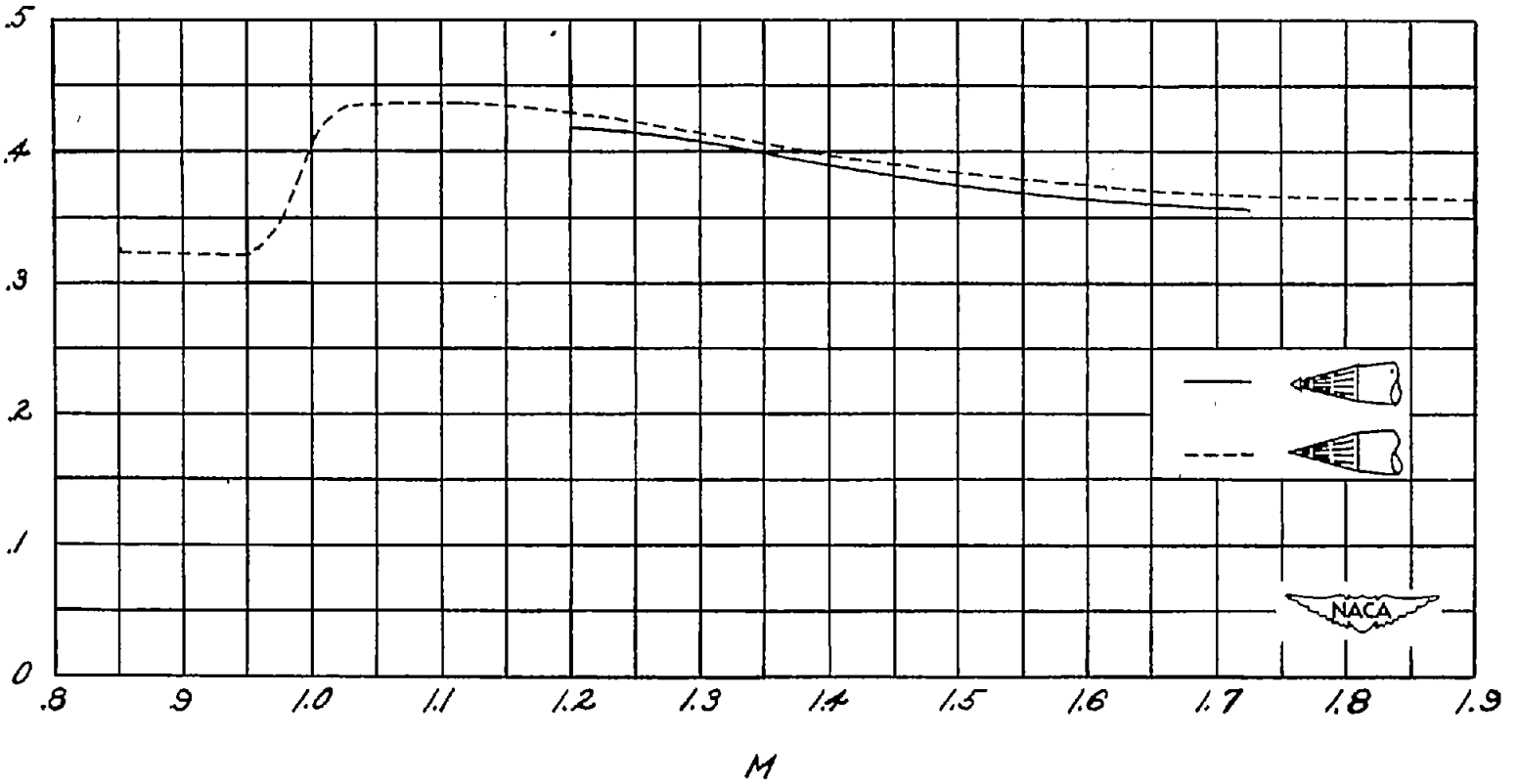

Figure 11.- Drag coefficient based on body frontal area C_D plotted against Mach number M for models with the slotted-cone nose shape with and without a 40° windshield.

NACA-Langley - 12-9-52 - 350